Atomic-scale study of diffusion in A15 Nb_3Sn

Rémy Besson,* Sylvain Guyot,† and Alexandre Legris‡
Laboratoire de Métallurgie Physique et Génie des Matériaux, C.N.R.S. U.M.R. 8517, Université des Sciences et Technologies de Lille, Bâtiment C6, 59655 Villeneuve d'Ascq Cedex, France

(Received 13 February 2006; revised manuscript received 1 December 2006; published 8 February 2007)

The point defect and diffusion properties of A15 Nb_3Sn are investigated using *ab initio* density functional theory calculations and statistical thermodynamics. The defect structure is found to be of antisite type, with small amounts of Nb vacancies, and Sn vacancies showing a trend towards instability. Diffusion occurs mainly on the Nb-sublattice (restricted to intrachain jumps for both species), Sn-sublattice exchanges being unlikely for both species. In addition, ordering (disordering) is found to occur via Sn (Nb) jumps. The calculated Nb and Sn tracer diffusion coefficients exhibit a low sensitivity to the alloy composition around stoichiometry at 1000 K, with $D^*_{Nb} \gg D^*_{Sn}$ provided the correlation between atomic jumps is taken into account. Agreement with interdiffusion measurements is reached with reasonably low values for the geometrical correlation factor.

DOI: 10.1103/PhysRevB.75.054105 PACS number(s): 61.72.−y, 66.30.−h, 31.15.Ar

I. INTRODUCTION

A15 Nb_3Sn is reputedly one of the best candidates for the development of superconducting wires,[1] in the context of the current researches on thermonuclear fusion (ITER project). Increasing the performances of these wires, however, requires the improvement of the elaboration processes, which implies a better understanding of the diffusion phenomena that occur during the growth of the intermetallic compound (at temperatures around 1000 K). To this aim, a reliable description of the point defect structure of Nb_3Sn is thus needed, all the more as the superconducting properties (critical temperature) of A15 alloys are also known to be extremely sensitive to point defects (especially antisite atoms[2]) through defect-induced local modifications of lattice relaxation times.[3,4] In particular, the critical temperature of A15 compounds strongly increases with the degree of long-range order, which is ordinarily maximum at stoichiometry.[5]

Experiments performed on Nb_3Sn have already yielded some valuable results about its point defect structure. Measurements of ordering kinetics,[6] assuming that the reordering rate of Nb is much slower than that of Sn, have allowed one to get an energy value $\simeq$2.6 eV for the activation of diffusion in Nb_3Sn, with similar values in other A15 compounds such as Nb_3Ge.[7] Such kinetic approaches, however, use point defect formation energies in a somewhat generic manner, without reference to the vacancy type or to the alloy local chemistry, and the link between point defects and alloy composition therefore needs more detailed investigations.

From a theoretical point of view, previous calculations with empirical pair potentials[8–10] have also provided information about point defects in Nb_3Sn, especially regarding the role of vacancies and the relative diffusivities of both elements, but the predictive ability of such approaches was limited by the use of pair interactions. Besides these empirical simulations, investigations combining analytical models with kinetic Monte Carlo calculations have proved to be efficient in giving quite general expressions and trends for tracer diffusion coefficients[11] and their relation with interdiffusion,[12] as well as evaluations of the correlation factors. However, involving models parametrized with various jump frequencies, these approaches cannot yield realistic values for the diffusion coefficients.

In this context, the increased confidence in *ab initio* energy calculations (density-functional theory[13,14]) has entailed in the last decades several structural and thermodynamic studies of point defects in metals and alloys, by combination with statistical models relying on an independent-defect (ID) approximation, using either the canonical[15,16] or grand canonical[17,18] equivalent descriptions. These models have been applied to binary intermetallic compounds (mainly AlM with M=Ni, Fe, or Ti—for a review, see, for instance, Ref. 19), and to a much lesser extent to some ternary systems (binary ordered alloys with additional elements).[20–22] Although restricted to small departures from stoichiometry, and thus intrinsically more limited than cluster approaches allowing a thermodynamic analysis on the whole composition range,[23] the ID description, however, constitutes a tractable and sound basis to tackle diffusion properties[24] in ordered compounds, provided (i) the mechanisms only involve vacancy-atom exchanges (no collective movements) and (ii) the binding between point defects is negligible (although the ID approach can easily be extended to take into account complex point defects).

As regards diffusion properties in concentrated alloys, few works have been published up to now. A thorough determination of the interdiffusion coefficient in disordered fcc-based Al-Li is presented in Ref. 25, while studies on ordered alloys remain partial, covering mainly B2 NiAl (Refs. 26 and 27) [and FeAl (Ref. 28)] and focusing on migration energies without assessment of overall diffusivities. For an ordered compound, the task of reaching macroscopic diffusion properties from atomic-scale parameters is therefore still incomplete.

In order to contribute to fill this gap, the purpose of the present paper is to thoroughly describe the method yielding (by means of *ab initio* atomic-scale calculations coupled with a statistical thermodynamic approach) the diffusion coefficients from atomic parameters in an ordered compound, and to apply it to A15 Nb_3Sn. This approach is all the more justified since it offers a way to get a deeper insight into experimentally intricate parameters such as the influence of off-stoichiometry, which should be essential owing to the

observed[29,30] composition gradients in growing Nb_3Sn layers.

II. METHODS

A. Energy calculations

The energy calculations were performed with the VASP software[31–34] (using density functional theory with plane waves and ultrasoft pseudopotentials) on a supercell containing 64 atoms ($2\times2\times2$ Nb_6Sn_2 unit cells) in periodic boundary conditions. Preliminary magnetic calculations (not reported here) on Nb, Sn, and Nb_3Sn perfect crystals systematically led to negligible total magnetic moments (below 2×10^{-3} μ_B/atom), in agreement with experiments describing Nb_3Sn as a nonmagnetic compound. The present study was therefore concerned merely with nonmagnetic calculations, assuming that no local magnetic moments exist around point defects. In each of the local density approximation (LDA)[35] and generalized gradient approximation (GGA)[36] (nonmagnetic) frameworks, four types of calculations were performed, according to the electrons explicitly taken into account in the pseudopotentials, namely (i) for Nb, either with only the $5s^24d^3$ electrons (five electrons, "Nb *sd*" pseudopotential) or including the $4p^6$ ones (11 electrons, "Nb *spd*"), and (ii) for Sn, either with only the $5s^25p^2$ electrons (4 electrons, "Sn *sp*") or including the $4d^{10}$ ones (14 electrons, "Sn *spd*"). The relevance of *a priori* taking into account the sensitivity of the results to the pseudopotentials was justified by the existence of such an effect when including addition elements such as Ta.[30] The sampling of the first Brillouin zone was performed through a $4\times4\times4$ mesh, and the cutoff energy for the plane-wave expansions was 260 eV, leading to a sufficient total energy convergence of 1 meV/atom. The jump paths were calculated using the nudged elastic band (NEB) method,[37] providing a reasonable assessement of the saddle-points. Finally, it should be noted that, whereas all point defect calculations allowed the relaxation of atomic positions and cell vectors, the migration energies were calculated at constant cell shape, the influence of pressure on migration profiles being negligible (less than 0.05 eV).

B. Point defect thermodynamics and diffusion

Using the foregoing energy calculations, the grand canonical (GC) energies of the various point defects (d) can be deduced according to the following relation:

$$E_{GC}(d) = E(d) - E_0, \tag{1}$$

with $E(d)$ the total energy of the supercell with defect d and E_0 the reference energy (undefected supercell). Under the assumption of noninteracting point defects, GC energies are then the basic quantities determining the point defect structure and thermodynamics of an ordered compound as a function of temperature and composition, through a statistical thermodynamic treatment either in isothermal-isobaric (NPT) or in GC (μVT)[18,20] formalism (the latter being adopted in the present work). The thermodynamic properties (alloy composition, point defects) are then functions of the chemical potentials, and the point defect formation energies read

$$E_f(d) = E_{GC}(d) + \delta\mu(d), \tag{2}$$

where $\delta\mu(d)$ is a linear combination of the chemical potentials μ_i (with integer coefficients) characteristic of defect d [for example, $\delta\mu(\mathrm{Sn_{Nb}})=\mu_{\mathrm{Nb}}-\mu_{\mathrm{Sn}}$ and $\delta\mu(V_{\mathrm{Nb}})=\mu_{\mathrm{Nb}}$; symmetric expressions hold for $\mathrm{Nb_{Sn}}$ and V_{Sn}; see below for defect notation].

Except the interstitial ones (neglected owing to the large atomic radii of Nb and Sn), all the simple (i.e., one-center) point defects were taken into account in the present investigation, namely antisite defects (Nb_{Sn}, Sn_{Nb}) and vacancies (V_{Nb}, V_{Sn}). The subscript refers to the sublattice on which each point defect occurs (the A15 structure consisting of six equivalent Nb sites and two Sn ones in each Nb_6Sn_2 cell).

The tracer diffusion coefficient of a chemical species A was calculated using the expression[38]

$$D_A^{\alpha\beta*} = \frac{1}{2} f_A^{\alpha\beta} \sum_m \Gamma_A(m) \sum_{k=1}^{K(m)} \delta r^\alpha(m,k)\,\delta r^\beta(m,k), \tag{3}$$

with $\Gamma_A(m)$ the frequency for jumps of type m [the inner sum running over the $K(m)$ equivalent jumps $\{\delta r^\alpha(m,k)\}_{1\leqslant\alpha\leqslant3}$ of type m] and $f_A^{\alpha\beta}$ the atomic correlation factor (in the case of the cubic A15 structure, $D_A^{\alpha\beta*}\neq0$ only for $\alpha=\beta$ and $D_A^*\hat{=}D_A^{\alpha\alpha*}$, $\forall\,\alpha$). For a vacancy-atom exchange mechanism involving two sublattices 1 and 2 in a system with I chemical species and R sublattices, the jump frequency of an A atom is given by the relation

$$\Gamma_A^{1\to2} = \frac{x_A^1 x_V^2}{\sum_I \sum_R x_A x_i^r k^r}\,\gamma_A^{1\to2}, \tag{4}$$

where x_A is the atomic fraction of species A, x_i^r is the site fraction of sublattice r occupied by species i (V=vacancy), k^r is the number of sites of type r per unit cell, and $\gamma_A^{1\to2}$ is the vacancy jump frequency for exchange with an A atom in a $1\to2$ jump, given by the relation from activated state theory:

$$\gamma_A^{1\to2} = \nu_A^{1\to2} e^{-E_A^{1\to2}/k_BT}, \tag{5}$$

$\nu_A^{1\to2}$ and $E_A^{1\to2}$ being, respectively, the attempt frequency and activation energy of the jump. In principle, the vibrational entropies should also be taken into account when assessing the point defect structure and diffusion properties, since the attempt frequencies in general depend on the type of jump and may thus range over several orders of magnitude. However, this procedure, relatively easy with empirical potentials,[27] becomes too difficult when *ab initio* methods are used. Therefore postponing for the future more precise calculations involving point defect and saddle-point entropies, the present work was performed with a single generic value (12 THz, a reasonable value for metallic systems) for the attempt frequencies.

TABLE I. Reference (undefected $2\times2\times2$ Nb_6Sn_2 supercell) and grand canonical energies (eV) of point defects in A15 Nb_3Sn, for each set of Nb and Sn pseudopotentials (nonmagnetic LDA and GGA approximations).

	LDA				GGA			
	Nb *sd* Sn *sp*	Nb *spd* Sn *sp*	Nb *sd* Sn *spd*	Nb *spd* Sn *spd*	Nb *sd* Sn *sp*	Nb *spd* Sn *sp*	Nb *sd* Sn *spd*	Nb *spd* Sn *spd*
Reference	−78.88	−77.32	−78.85	−77.27	−70.24	−69.07	−70.19	−69.04
V_{Nb}	13.37	13.14	13.38	13.13	12.02	11.79	12.02	11.79
V_{Sn}	8.75	9.03	8.75	9.01	7.87	7.92	7.85	7.91
Nb_{Sn}	−6.46	−6.16	−6.47	−6.18	−6.11	−5.90	−6.13	−5.91
Sn_{Nb}	6.96	6.73	7.00	6.77	6.60	6.39	6.56	6.43

From tracer diffusion properties, the chemical (or interdiffusion) coefficient is then given by the Darken-Manning relation (for example[38]):

$$\tilde{D} = (x_{Nb}D^*_{Sn} + x_{Sn}D^*_{Nb})\phi S \tag{6}$$

with

$$\phi = \frac{1}{k_BT}\frac{\partial\mu_{Nb}}{\partial \ln x_{Nb}} = \frac{1}{k_BT}\frac{\partial\mu_{Sn}}{\partial \ln x_{Sn}} \tag{7}$$

the "thermodynamic factor" (μ_i being the chemical potential of species i), and S the "vacancy wind" factor, given by[39]

$$S = 1 + \frac{(1-f_0)x_{Nb}x_{Sn}(D^*_{Nb} - D^*_{Sn})^2}{f_0(x_{Nb}D^*_{Nb} + x_{Sn}D^*_{Sn})(x_{Nb}D^*_{Sn} + x_{Sn}D^*_{Nb})} \tag{8}$$

with f_0 the geometrical tracer correlation factor[40] for self-diffusion in a pure crystal with the A15 structure, which has to be distinguished from the tracer correlation factors entering in relation (3).

III. RESULTS

A. Point defect structure

The LDA and GGA point defect GC energies in Nb_3Sn are displayed in Table I for the four possible combinations of Nb and Sn pseudopotentials. As these quantities pertain to defected systems with locally different compositions, no conclusions regarding the relative stabilities of the defects can be drawn from their direct comparison. From Table I, it, however, appears clearly that including the *d* electronic shell in the Sn pseudopotential is immaterial, whereas the *p* electrons in the Nb pseudopotential induce energy variations up to 0.3 eV. Nevertheless, the influence of the Nb *p* shell on thermodynamic properties (defect formation energies) was found negligible throughout, and we therefore concentrate in the following on those results obtained with the Nb *sd* and Sn *sp* pseudopotentials.

From the GC energies, the point defect structure of Nb_3Sn at $T=300$ K around A15 stoichiometry was calculated using the Nb *sd* and Sn *sp* pseudopotentials in LDA and GGA [Fig. 1(a)], the fraction of a given point defect being defined as the ratio between the number of such defects and the number of sites of the corresponding sublattice. At room temperature, the compound almost exclusively contains antisites, the amounts of both kinds of vacancies being completely negligible. Sn vacancies have a very high (4 eV) formation energy on both sides of stoichiometry, while that of Nb vacancies, although significant, lies below 2 eV [Fig. 1(b)]. In agreement with results obtained in pure metals[41] and intermetallics,[42] the calculated vacancy formation energies are slightly higher in LDA than in GGA.

Calculations at 1000 K (temperature used in the subsequent diffusion study, Fig. 2) show that on a wide range of temperature, Nb_3Sn remains an antisite compound, with Nb vacancies as secondary defects and negligible amounts of Sn vacancies. These defects (V_{Nb} and V_{Sn}) may, however, play a role in diffusion, provided the activation barriers are low enough. Moreover, the influence of the DFT framework on the point defect structure is limited, the LDA and GGA approaches showing for the various sets of pseudopotentials a remarkable agreement about antisite atoms, together with a weak dispersion as regards the amounts of vacancies (as stressed above, the results of Fig. 2 hold for all pseudopotentials). This noticeable coherence deserves emphasizing since this is by no means of general validity when comparing the respective merits of the LDA and GGA for an ordered compound.[43] Our results also clearly show that Nb_3Sn accommodates the off-stoichiometry at room temperature with only one kind of antisite defect, the mixing of the chemical species on both sublattices occurring only at higher temperatures. This behavior significantly differs from that obtained

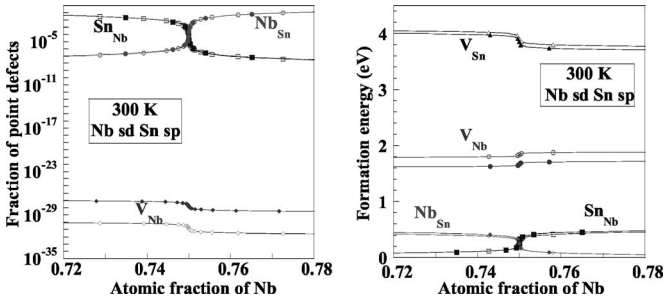

FIG. 1. Point defect (a, left) structure and (b, right) formation energies (eV) in Nb_3Sn at 300 K around A15 stoichiometry, calculated with the Nb *sd* and Sn *sp* pseudopotentials in the nonmagnetic LDA and GGA frameworks (open and closed symbols, respectively).

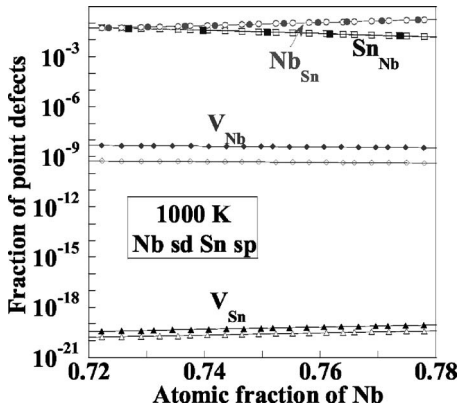

FIG. 2. Point defect structure of Nb_3Sn at $T=1000$ K, calculated with the *sd* pseudopotential for Nb (LDA and GGA: open and closed symbols, respectively).

in A15 Nb_3Au from x-ray diffraction experiments[44] pointing out roughly equivalent amounts of Nb_{Au} and Au_{Nb} in $Nb_{2.98}Au_{1.02}$ at room temperature.

B. Diffusion properties

Because of the low sensitivity of the point defect structure to the pseudopotentials and exchange-correlation approximation used, the diffusion study was carried out merely within the (LDA, Nb *sd*, Sn *sp*) framework, since (i) this restriction should not be critical (as indicated by the noticeable coherence of the point defect properties predicted by the various density functional theory formalisms), and (ii) the LDA has shown to be the best available scheme to describe vacancies in pure metals[41] and probably also in ordered alloys.[42] A more critical point, however, concerns the elementary diffusion mechanisms: although the diffusion processes in ordered compounds may be rather intricate (cycles,…), it is of interest to get information about the importance of elementary mechanisms involving a single atom-vacancy exchange, especially since collective movements are not expected in Nb_3Sn.[9] In this framework, our investigation of the diffusion properties in the compound was led by considering the shortest jumps between each couple of sublattices (Fig. 3), namely (i) ordering/disordering jumps involving both sublattices, (ii) Sn-sublattice jumps, and (iii) Nb-sublattice jumps, the latter being divided into intrachain and interchain ones. The migration energy paths represented in Fig. 4 indicate the

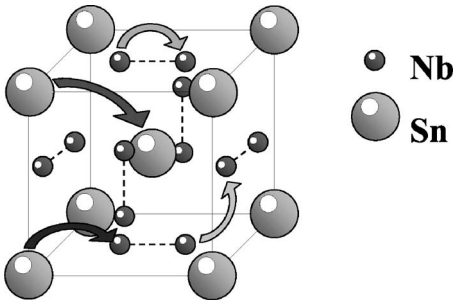

FIG. 3. A15 structure and atomic jumps considered in the present work.

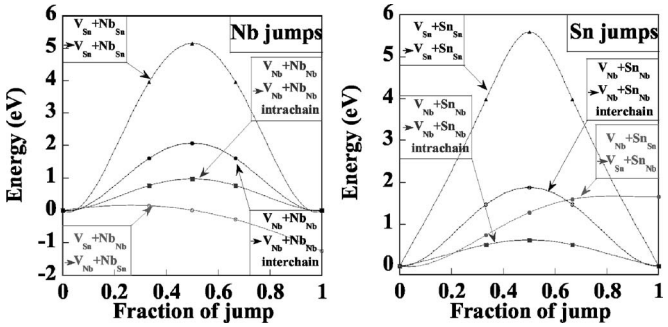

FIG. 4. Kinetic paths corresponding to Fig. 3 for (a, left) Nb and (b, right) Sn atoms in A15 Nb_3Sn (nonmagnetic LDA calculations with Nb *sd* and Sn *sp* pseudopotentials). Lines are visual guides.

low stabilities (i) of the Sn vacancy with respect to the $[V_{Nb}+Nb_{Sn}]$ complex defect, and conversely (ii) of the $[V_{Sn}+Sn_{Nb}]$ complex defect with respect to the Nb vacancy. However, since none of these defects was strictly found to be unstable, the corresponding profiles were taken into account in evaluating the diffusion coefficients. It is worth mentioning that the pathways connecting both sublattices suggest a dissymetric role of the chemical species in Nb_3Sn, ordering (disordering) proceeding by Sn jumps (Nb), in agreement with usual assumptions involving atomic movements between wrong and right sublattices.[7]

As regards intrasublattice jumps, the main features are (i) the large discrepancy in the barrier heights between jumps within the Sn sublattice and those within the Nb sublattice (the latter being much easier than the former ones), and (ii) within the Nb sublattice the definite preference for intrachain jumps for both species. The numerical values of the various migration energies involved are listed in Table II, giving rise to a kinetic model with ten frequencies calculated according to Eq. (5).

Knowing the equilibrium concentrations of chemical species and vacancies, the atomic jump rates [Eq. (4)] can then be calculated to yield the random tracer diffusion coefficients [Eq. (3) with $f_A^{\alpha\beta}=1$]. The tracer correlation factors, which may range on several orders of magnitude (between 0 and 1) in ordered compounds, were determined separately using the calculated exchange frequencies [Eq. (5)] as input parameters of an analytic model devised for A15 compounds.[11] The corresponding (random and actual) tracer diffusion coefficients are presented as a function of composition at $T=1000$ K in Fig. 5. As a first salient feature, neglecting

TABLE II. Migration energies (eV) of the jumps considered (nonmagnetic LDA calculations, Nb *sd* and Sn *sp* pseudopotentials; for intersublattice jumps, ord.=ordering and dis.=disordering).

	X=Nb	X=Sn
$V_{Nb}+X_{Nb}\rightarrow V_{Nb}+X_{Nb}$ intra.	0.98	0.62
$V_{Nb}+X_{Nb}\rightarrow V_{Nb}+X_{Nb}$ inter.	2.07	1.88
$V_{Sn}+X_{Sn}\rightarrow V_{Sn}+X_{Sn}$	5.15	5.59
$V_{Sn}+X_{Nb}\rightarrow V_{Nb}+X_{Sn}$	0.15 (dis.)	0.05 (ord.)
$V_{Nb}+X_{Sn}\rightarrow V_{Sn}+X_{Nb}$	1.41 (ord.)	1.70 (dis.)

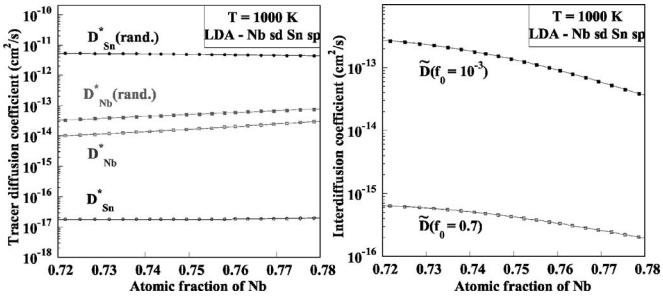

FIG. 5. Influence of atomic and geometrical correlation, respectively, on (a) tracer and (b) chemical (or inter-) diffusion coefficients in A15 Nb_3Sn at 1000 K in the atom-vacancy exchange mechanism (nonmagnetic LDA calculations with Nb *sd* and Sn *sp* pseudopotentials, using a generic 12 THz attempt frequency for all jumps).

correlation leads to $D^*_{Sn}(rand) \gg D^*_{Nb}(rand)$ by two orders of magnitude on both sides of stoichiometry, in disagreement with previous theoretical estimations (also neglecting correlation),[9] which points out the limited numerical accuracy of approaches relying on interatomic potentials. Moreover, the random tracer diffusion coefficients seem at odds with experimental conclusions[45] indicating a preferential Sn diffusion in grain boundaries rather than in the bulk.

The effect of correlation, quite limited for Nb, turns out to be dramatic for Sn, lowering the diffusion of this element by five orders of magnitude. The result $D^*_{Nb} \gg D^*_{Sn}$ then confirms the experimental conclusions as well as those of a previous numerical study including correlations but relying on generic values for the exchange frequencies.[11] Moreover, both diffusion coefficients smoothly vary with increasing Nb content, the composition dependence of D^* being slightly more sensitive for Nb than for Sn.

IV. DISCUSSION

From a theoretical point of view, the only available atomic-scale study of the point defect and diffusion properties of A15 Nb_3Sn was performed by computer simulations with pair potentials.[9] As concerns the point defect structure, and in spite of the limited accuracy of pair interactions, the conclusions of these authors remarkably agree with ours, both works pointing out an antisite-type compound, with vanishingly small amounts of vacancies. The unstable character of V_{Sn} found with empirical potentials corresponds to the roughly decaying profile of Fig. 4(a) in the present work (although we did not strictly find V_{Sn} to be unstable). The possible splitting of the Nb vacancy mentioned by these authors was, however, overlooked in the present work because this process implies supercell sizes beyond the current possibilities of *ab initio* methods.

As for diffusion properties, at variance with the present work [Fig. 5(a)], these authors obtain a bulk random Nb diffusion larger than the Sn one, a feature also pointed out by a theoretical work[11] including correlation (coupling analytical and Monte Carlo calculations). However, defining for each species γ^{ord}, γ^{intra}, γ^{inter}, and γ^{dis} to be, respectively, the ordering, intrachain exchange, interchain exchange, and disordering frequencies, it should be noted that our work provides a somewhat different hierarchy among the various jump frequencies from that assumed in Ref. 11, which also proves to be dependent on the chemical species, since we obtain $\gamma^{dis}(Nb) \gg \gamma^{intra}(Nb) \gg \gamma^{ord}(Nb) \gg \gamma^{inter}(Nb)$, and $\gamma^{ord}(Sn) \gg \gamma^{intra}(Sn) \gg \gamma^{dis}(Sn) > \gamma^{inter}(Sn)$. The available analytical investigations, although worthwhile in principle, may therefore deserve to be revisited taking into account a more realistic hierarchy between the jump frequencies, including the dissymetric roles of both species as regards the migration energies (especially the ordering/disordering ones).

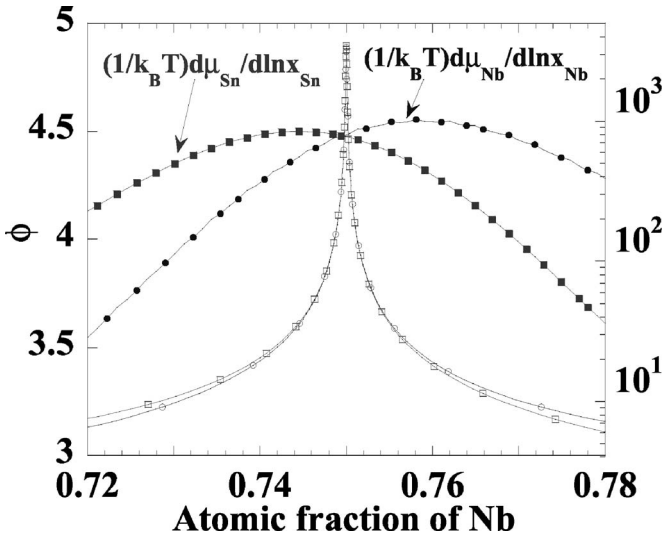

FIG. 6. Thermodynamic factors calculated (in LDA with Nb *sd* and Sn *sp*) at $T=1000$ K (closed symbols, left scale) and 300 K (open symbols, right scale) from Nb and Sn parameters (circles and squares, respectively); see text for explanations.

Completing the thermodynamic treatment of this work, the 1000 K and room temperature thermodynamic factors [required in $\tilde{D}$, Eq. (6) and (8)] were calculated from Eq. (7) within the ID approximation (Fig. 6) in LDA with Nb *sd* and Sn *sp*. Beside the strong temperature dependence of this quantity (implying marked effects on chemical diffusion), it should be noticed that the approximate treatment of the zero pressure condition in the ID model leads to results following only partially the Gibbs-Duhem relation [enabling one in principle to obtain ϕ either from μ_{Nb} or from μ_{Sn}, Eq. (7)]. Although this feature is more visible at high temperature, it is not critical for the present investigation on diffusion properties (the order of magnitude of ϕ being unaffected), and a unique value of 5 was subsequently adopted for ϕ at 1000 K at any composition around stoichiometry.

For purpose of comparison with experimental results, the interdiffusion coefficient $\tilde{D}$ [Fig. 5(b)] was calculated at 1000 K from D^* [Eq. (6)]. In using Eq. (6), an uncertainty lies in the choice of the geometrical correlation factor f_0, as its value remains ambiguous in the literature. In order to illustrate its influence, the calculation of the interdiffusion coefficient was therefore performed with two limiting trial values for f_0: 0.7 (characteristic of common cubic structures) and 10^{-3} (in agreement with the work of Ref. 12 which sug-

gests $f_0 \ll 1$). Within this range of values for f_0, $\tilde{D}$ appears to be roughly inversely proportional to this parameter, a behavior that could not be directly deduced from Eq. (8) without the explicit calculation of D^*. Whatever the f_0 value, $\tilde{D}$ shows a noticeable decrease with increasing Nb content. The lower value for f_0 gives calculated results in better agreement with experimental values $(5 \times 10^{-13}\ \mathrm{cm}^2/\mathrm{s})$ for interdiffusion.[46]

Previous investigations[12] have shown that the correlation factor f_0 for the interdiffusion coefficient is a function of the ratio $\gamma^{inter}/\gamma^{intra}$ between the interchain and intrachain jump frequencies. Our study leads for $\gamma^{inter}/\gamma^{intra}$ to values between 10^{-6} and 10^{-5} for both Nb and Sn, respectively, at 1000 K, which reflects the fact that the intrachain jumps are strongly favored with respect to the interchain ones, and should lead to f_0 values close to zero.[12] This conclusion is confirmed by the agreement (with $f_0 = 10^{-3}$) between our calculations [Fig. 5(b)] and the available experimental value of $\tilde{D}$ $(5 \times 10^{-13}\ \mathrm{cm}^2/\mathrm{s}$ at 1000 K).[46] The comparison between theory and experiment could be drawn further by use of kinetic Monte Carlo methods, allowing more precise assessment of diffusion correlation factors.[25]

Our calculations also shed new light on previous experiments and models about the ordering kinetics of Nb_3Sn:[5,6] these models hinge on mixed jumps involving both sublattices, and should thus be refined in order to take into account the species-dependent ordering and disordering mechanisms. Moreover, the agreement is correct between the activation energy for diffusion obtained from kinetics measurements (2.58 eV) and the present one ($\simeq$2.8 eV), obtained for Nb by adding the migration (0.98 eV, Table II) and vacancy formation energies [$\simeq$1.8 eV, Fig. 1(b)].

Finally, in polycrystalline Nb_3Sn, our results are consistent with the possibility of Sn diffusion mediated by grain boundaries (as observed experimentally[45]). Supposing that diffusion mainly occurs (i) for Nb in the bulk and (ii) for Sn in grain boundaries (GB, the bulk component being negligible[45,47]), the interdiffusion coefficient [given by relation (6) in which therefore $D^*_{Nb} = D^*_{Nb}(bulk)$ and $D^*_{Sn} = D^*_{Sn}(GB)$] reads $\tilde{D} \simeq D^*_{Nb}(bulk) + D^*_{Sn}(GB)$. Combining the experimental interdiffusion value $\tilde{D}(\mathrm{expt}) \simeq 5 \times 10^{-13}\ \mathrm{cm}^2/\mathrm{s}$ (Ref. 46) with the calculated $D^*_{Nb}(bulk)$ value $(10^{-14}\ \mathrm{cm}^2/\mathrm{s})$ hence yields $D^*_{Sn}(GB)$ possibly of the same order of magnitude.

Several refinements may be brought to this diffusion study. First, it was restricted to a single attempt frequency value (characteristic of phonon properties), whereas depending on the precise jump considered, this quantity may range in ordered alloys over several orders of magnitude, as recently shown by EAM calculations in Ni-Al.[27] Also, including the entropies (point defect formation[48] and saddle points) in the analysis might constitute a further improvement, but this task can hardly be achieved for the moment. Finally, according to investigations with pair potentials,[9] Nb vacancies may occur in a partial form along the Nb chains ("split-n vacancies" for two partial vacancies separated by n Nb atoms) and Sn vacancies are less stable than $[V_{Nb}+Nb_{Sn}]$ complexes. Our approach could thus be refined by taking into account the clustering between Nb_{Sn} and V_{Nb} antisite defects, especially $[V_{Nb}+Nb_{Sn}]$ (and perhaps five-center $[4V_{Nb}+Nb_{Sn}]$[9]) complexes. This point may, however, not be critical, since additional calculations (not shown here for brevity) indicate that the binding between point defects in Nb_3Sn should be low, at least for bidefects (the case of five-center defects should be treated separately with larger supercells).

V. CONCLUSION

The main purpose of this work was to describe the methodology leading from atomic-scale properties to macroscopic diffusivities in an ordered alloy, as well as to provide a reliable assessment of matter transport in A15 Nb_3Sn. Within the context of density-functional theory, the remarkable coherence between the results obtained in the LDA or GGA approaches and using different pseudopotentials for both chemical species should give our conclusions a sufficient level of confidence. As a first key point, Nb_3Sn essentially appears as an antisite compound, the density of vacancies (especially V_{Sn}) remaining negligible below the melting temperature. As regards transport properties, the main result is the significant tracer diffusivity of Nb, which lies three orders of magnitude above that of Sn, when the tracer correlation factors are taken into account. The movements of both species, occurring by Nb intrasublattice as well as intersublattice jumps, are therefore mediated by both types of vacancies. The dissymetric behavior of mixed (involving both sublattices) complexes, either stable or unstable with respect to isolated vacancies, indicates that the atomic mechanisms underlying the ordering kinetics should deserve further investigation. Finally, an adequate choice of the geometrical correlation factor provides a calculated interdiffusion coefficient in reasonable agreement with available experiments, suggesting that the jump mechanisms considered here (atom-vacancy exchanges) may be sufficient to correctly describe the bulk diffusion properties of Nb_3Sn. Our work finally supports the hypothesis of Nb_3Sn growth governed by bulk Nb and probably intergranular Sn diffusion mechanisms.

ACKNOWLEDGMENT

This work has benefited from the facilities of the C.R.I. U.S.T.L. supported by the Fonds Européen de Développement Régional.

*Corresponding author. Electronic address: remy.besson@univ-lille1.fr
†Electronic address: S.Guyot@ed.univ-lille1.fr
‡Electronic address: Alexandre.Legris@univ-lille1.fr

[1] *Intermetallic Compounds: Principles and Practice*, edited by J. H. Westbrook and R. L. Fleischer (Wiley, New York, 1994).
[2] A. R. Sweedler, D. G. Schweitzer, and G. W. Webb, Phys. Rev. Lett. **33**, 168 (1974).
[3] J. Labbé and J. Friedel, J. Phys. (France) **27**, 153 (1966).
[4] J. Labbé, S. Barišić, and J. Friedel, Phys. Rev. Lett. **19**, 1039 (1967).
[5] D. Dew-Hughes and T. S. Luhman, J. Mater. Sci. **13**, 1868 (1978).
[6] S. K. Agarwal and A. V. Narlikar, Solid State Commun. **55**, 563 (1985).
[7] D. Dew-Hughes, J. Phys. Chem. Solids **41**, 851 (1980).
[8] N. V. Moseev, V. G. Chudinov, B. N. Goshchitskii, and V. I. Protasov, Phys. Status Solidi A **79**, 67 (1983).
[9] D. Welch, G. J. Dienes, O. W. Lazareth, Jr., and R. D. Hatcher, J. Phys. Chem. Solids **45**, 1225 (1984).
[10] N. V. Moseev, V. G. Chudinov, B. N. Goshchitskii, and V. I. Protasov, Phys. Status Solidi A **94**, 147 (1986).
[11] I. V. Belova and G. E. Murch, J. Phys. Chem. Solids **58**, 1383 (1997).
[12] I. V. Belova and G. E. Murch, J. Phys. Chem. Solids **60**, 2023 (1999).
[13] P. Hohenberg and W. Kohn, Phys. Rev. **136**, B864 (1964).
[14] W. Kohn and L. J. Sham, Phys. Rev. **140**, A1133 (1965).
[15] Y. Mishin and D. Farkas, Philos. Mag. A **75**, 169 (1997).
[16] M. Hagen and M. W. Finnis, Acta Mater. **77**, 447 (1998).
[17] C. L. Fu, Y. Y. Ye, M. H. Yoo, and K. M. Ho, Phys. Rev. B **48**, 6712 (1993).
[18] J. Mayer, C. Elsasser, and M. Fahnle, Phys. Status Solidi B **191**, 283 (1995).
[19] Y. Mishin and C. Herzig, Acta Mater. **48**, 589 (2000).
[20] C. L. Fu and J. Zou, Acta Mater. **44**, 1471 (1996).
[21] C. Woodward, S. Kajihara, and L. H. Yang, Phys. Rev. B **57**, 13459 (1998).
[22] C. Woodward and S. Kajihara, Acta Mater. **47**, 3793 (1999).
[23] F. Lechermann and M. Fahnle, Phys. Rev. B **63**, 012104 (2000).
[24] M. Fahnle, Defect Diffus. Forum **203-205**, 37 (2002).
[25] A. VanderVen and G. Ceder, Phys. Rev. Lett. **94**, 045901 (2005).
[26] Y. Mishin and D. Farkas, Philos. Mag. A **75**, 187 (1997).
[27] A. Y. Lozovoi and Y. Mishin, Phys. Rev. B **68**, 184113 (2003).
[28] M. Fahnle, J. Mayer, and B. Meyer, Intermetallics **7**, 315 (1999).
[29] P. J. Lee and D. C. Larbalestier, IEEE Trans. Appl. Supercond. **11**, 3671 (2000).
[30] S. Guyot, Ph.D. thesis, UST Lille, Villeneuve d'Ascq-France, 2005.
[31] G. Kresse and J. Hafner, Phys. Rev. B **47**, 558 (1993).
[32] G. Kresse and J. Hafner, Phys. Rev. B **49**, 14251 (1994).
[33] G. Kresse and J. Furthmuller, Phys. Rev. B **54**, 11169 (1996).
[34] G. Kresse and J. Furthmuller, Comput. Mater. Sci. **6**, 15 (1996).
[35] J. P. Perdew and A. Zunger, Phys. Rev. B **23**, 5048 (1981).
[36] J. P. Perdew and Y. Wang, Phys. Rev. B **45**, 13244 (1991).
[37] G. Mills, H. Jonsson, and G. K. Schenter, Surf. Sci. **324**, 305 (1995).
[38] *Atomic Transport in Solids*, edited by A. R. Allnatt and A. B. Lidiard (Cambridge University Press, Cambridge, England, 1993).
[39] J. R. Manning, *Diffusion Kinetics for Atoms in Crystals* (Van Nostrand, Princeton, NJ, 1968).
[40] A. B. Lidiard, Acta Metall. **34**, 1487 (1986).
[41] T. R. Mattsson and A. E. Mattsson, Phys. Rev. B **66**, 214110 (2002).
[42] R. Besson, A. Legris, and J. Morillo, Phys. Rev. B **74**, 094103 (2006).
[43] F. Lechermann, F. Welsch, C. Elsasser, C. Ederer, M. Fahnle, J. M. Sanchez, and B. Meyer, Phys. Rev. B **65**, 132104 (2002).
[44] V. E. Antonov, E. L. Bokhenkov, B. Dorner, V. K. Fedotov, G. Grosse, A. L. Latynin, F. E. Wagner, and R. Wordel, J. Alloys Compd. **264**, 1 (1998).
[45] C. Verwaerde, Ph.D. thesis, UST Lille, Villeneuve d'Ascq-France, 1996.
[46] B. A. Glowacki and J. E. Evetts, IEEE Trans. Magn. **25**, 2200 (1989).
[47] D. J. Rodrigues, C. L. H. Thieme, D. G. Pinatti, and S. Foner, IEEE Trans. Appl. Supercond. **5**, 1607 (1995).
[48] J. Mayer and M. Fahnle, Acta Mater. **45**, 2207 (1997).